

Document Version

Final published version

Citation (APA)

Zamparete, R., & Makinwa, K. (2023). A 720 nW Current Sensor with 0-to-15 V Input Common-Mode Range and $\pm 0.5\%$ Gain Error from -40 to 85 °C. In *Proceedings of the 2023 IEEE Symposium on VLSI Technology and Circuits, VLSI Technology and Circuits 2023* (Digest of Technical Papers - Symposium on VLSI Technology; Vol. 2023-June). IEEE. <https://doi.org/10.23919/VLSITechnologyandCir57934.2023.10185309>

Important note

To cite this publication, please use the final published version (if applicable).
Please check the document version above.

Copyright

In case the licence states "Dutch Copyright Act (Article 25fa)", this publication was made available Green Open Access via the TU Delft Institutional Repository pursuant to Dutch Copyright Act (Article 25fa, the Taverne amendment). This provision does not affect copyright ownership.
Unless copyright is transferred by contract or statute, it remains with the copyright holder.

Sharing and reuse

Other than for strictly personal use, it is not permitted to download, forward or distribute the text or part of it, without the consent of the author(s) and/or copyright holder(s), unless the work is under an open content license such as Creative Commons.

Takedown policy

Please contact us and provide details if you believe this document breaches copyrights.
We will remove access to the work immediately and investigate your claim.

Green Open Access added to TU Delft Institutional Repository

'You share, we take care!' - Taverne project

<https://www.openaccess.nl/en/you-share-we-take-care>

Otherwise as indicated in the copyright section: the publisher is the copyright holder of this work and the author uses the Dutch legislation to make this work public.

A 720 nW Current Sensor with 0-to-15 V Input Common-Mode Range and $\pm 0.5\%$ Gain Error from -40 to 85°C

Roger Zamparete¹, Kofi Makinwa¹

¹Delft University of Technology, Delft, The Netherlands

Abstract

This paper presents a nano-power high-side shunt-based current sensor (CS) that digitizes the voltage drop across an on-chip ($\pm 1\text{A}$) or a lead-frame ($\pm 30\text{A}$) shunt. A TC-tunable ADC reference compensates for the shunts' large temperature coefficient (TC), resulting in $\pm 0.5\%$ gain error from -40 to 85°C . The CS employs a capacitively coupled g_m -boosted front-end followed by a CCO-based $\Delta\Sigma$ ADC. Together with a floating input chopper, this results in an input common-mode range (ICMR) of 0-to-15V, the largest reported for a CS implemented in a standard CMOS process. It achieves high energy efficiency (164dB FoM) while consuming only 720nW, representing a 4 \times improvement on the state-of-the-art and making this the first ever reported sub- μW smart current sensor.

Introduction

Knowing the battery State of Charge is essential for the reliable operation of IoT devices, and it is typically determined by Coulomb counting. Since it must always be on, this requires a low-power CS [1-4], which, for IoT applications, should also be low-cost. The latter can be achieved using metal shunts, such as on-chip, lead-frame, and PCB traces, but their readout circuits often consume several μW s, significantly impacting battery life. High-side sensing is preferred, but it is an extra challenge in multi-cell battery applications and typically requires an expensive BCD process [3,4]. This work proposes a nano-power high-side CS compatible with low-cost metal shunts and fabricated in a standard $0.18\mu\text{m}$ CMOS process.

Proposed Current Sensor

As shown in Fig.1a, the CS employs an ADC with a TC-tunable $V_{\text{REF}}=V_{\text{PTAT}}\pm\lambda\cdot V_{\text{CTAT}}$ [2] to digitize the voltage across a metal shunt $V_S = R_S I_S$ while simultaneously compensating for its 1st-order TC (~ 3500 ppm/ $^\circ\text{C}$). The CS can be used with either a lead-frame shunt ($300\mu\Omega$, $\pm 30\text{A}$, Fig.1b) or an on-chip metal shunt ($40\text{m}\Omega$, $\pm 1\text{A}$, Fig.1c) [2,4].

Previous TC-tunable V_{REF} generators used separate circuits for V_{PTAT} and V_{CTAT} [1,2]. In this work, V_{REF} is generated by a single circuit to save power (Fig. 2). The PTAT voltage across a dynamic threshold MOST (DTMOST) pair is added to a CTAT voltage $I_{\text{BIAS}}\lambda\cdot R_{\text{CTAT}}$, where λ is a trim factor. The use of DTMOSTs instead of BJTs enables $V_{\text{DD}}<1\text{V}$ since V_{SG} (250mV @ 25°C) is $\sim 3\times$ smaller than V_{BE} (700mV @ 25°C). However, a low-TC bias current I_{BIAS} is required to minimize the non-linear temperature dependence of the resulting V_{REF} .

As shown in Fig. 3, I_{BIAS} is generated by forcing the PTAT voltage produced by a DTMOST pair across a silicided poly resistor (R_{SIL}), whose near-PTAT TC results in a near-zero TC current. This is realized by a current-voltage mirror (CVM) [5] rather than the usual opamp, saving power and enabling $V_{\text{DD}}<1\text{V}$. The current is then mirrored to another DTMOST pair in series with two 4-bit resistor ladders, R_{MSB} ($R_{\text{UNIT}}=8\text{k}\Omega$) and R_{LSB} ($R_{\text{UNIT}}=0.5\text{k}\Omega$) that realize the TC-tuning. A polarity bit λ_{PN} selects the appropriate ladder, resulting in a 9-bit trim DAC using just 34 switches, thus significantly reducing switch leakage while providing accurate Kelvin connections. The CVM and mirrors are chopped at $f_{\text{CH}}=f_s/2$ to suppress offset/flicker noise.

As shown in Fig. 4, V_S is sensed by a capacitively-coupled g_m stage, which is chopped at $f_{\text{CH}}=f_s/2$, thus suppressing its

offset/flicker noise and decoupling the DC levels of the input and the $\Delta\Sigma$ summing node. System-Level Chopping (SLC) further suppresses offset with $f_{\text{SLC}} = f_s/64$. The floating input choppers [4] are protected by a custom ESD structure, which enables a high ICMR ($<15\text{V}$). Using a 1st-order $\Delta\Sigma$ ensures a uniform impulse response [2], but its finite DC gain leads to dead zones and low SQNR. A phase quantizing loop filter based on two current-controlled oscillators (CCOs) is employed to address these issues. It provides multi-bit quantization and high DC gain, even for $V_{\text{DD}}<1\text{V}$ [6]. A phase frequency detector (PFD) quantizes the CCOs' phase difference, resulting in a 4-bit, 3-level output that drives a capacitive DAC C_{DAC} . Compared to [6], the middle level is obtained by simply shorting the bottom plates of C_{DAC} . Finally, dead-banding (DB) suppresses chopping-induced non-linearity [7].

For energy efficiency, the bias current of the g_m stage also supplies the CCOs ($I_{\text{CCOP(N)}}$) (Fig.5). Large loop-gain ($\propto g_m\cdot k_{\text{CCO}}$) is required for high SQNR, while reducing k_{CCO} reduces f_{CCO} and dynamic power consumption. A current-reuse g_m -boosting scheme is proposed to decouple the g_m choice from the I_{CCO} . The cross-coupled M_{boost} transistors create a negative g_m that boosts the effective g_m (g_{meff}) to, ideally, infinity. The series resistors R_S stabilize the system and define $g_{\text{meff}}=1/R_S=4\mu\text{S}$ ($\sim 3\times$ the g_m of M_{gm}) with $I_{\text{CCOP(N)}}=60\text{nA}$ and $f_{\text{CCO}}=16\text{kHz}$. They also provide pseudo-differential degeneration, leading to a wider input range. A large bias resistor $R_B=5\text{G}\Omega$ is required to minimize its noise contribution, which is realized as a Segmented Duty-Cycled Resistor (SDCR) [1] operating at $f_{\text{SDCR}} = f_s$.

Measurement Results and Performance Summary

The CS is fabricated in a standard $0.18\mu\text{m}$ CMOS process (Fig.6a) and consumes 720nW from a single 0.9V supply. The ADC achieves a $4\mu\text{V}_{\text{RMS}}$ resolution in a 5ms conversion time for $f_s=32\text{kHz}$. Decimation is performed off-chip for flexibility. The chip is shown in Fig 6b mounted on the lead-frame from a standard package.

Fig.7 shows ΔI_{OUT} vs. ΔV_{IN} of the g_m stage with and without g_m -boosting. As shown in Fig. 8, the lower quantization noise and increased gain with g_m -boosting increase the modulator's thermal-noise limited BW from $\sim 60\text{Hz}$ to $\sim 200\text{Hz}$. Fig. 9 and Fig. 11 show the D_{OUT} ($I_S=0.5\text{A}$, on-chip / $I_S=20\text{A}$, lead-frame) and I_{BIAS} variation from -40 to 85°C for a typical sample. The TC of $I_{\text{BIAS}}=140\text{ppm}/^\circ\text{C}$, and the on-chip/lead-frame D_{OUT} variation is $\pm 0.3\%/<0.5\%$. Fig.10 shows the gain error for the on-chip/ and lead-frame shunts (0.5%, four samples each) after a room temperature gain trim and a λ batch calibration. The spectrum for different ICMs is shown in Fig. 12, demonstrating the 0-to-15V ICMR. The offset stays below $100\mu\text{V}/5\mu\text{V}$ with SLC on/off for eight samples, as shown in Fig.13.

The sensor's performance is summarized in Tab.1. Compared to the state-of-the-art, it requires $\sim 4\times$ less power and is more energy efficient. Moreover, it supports high-side sensing up to 15V and is the first reported sub- μW CMOS current sensor.

References

- [1] Z. Tang, *et al.*, *ISSCC*, 2023.
- [2] R. Zamparete, *et al.*, *VLSI*, 2021.
- [3] C. Vroonhoven, *ISSCC*, 2020.
- [4] L. Xu, *et al.*, *ISSCC*, 2018.
- [5] K. Souri, *ISSCC*, 2014.
- [6] W. Zhao, *JSSC*, 2019.
- [7] H.Chandrakumar, *JSSC*, 2018

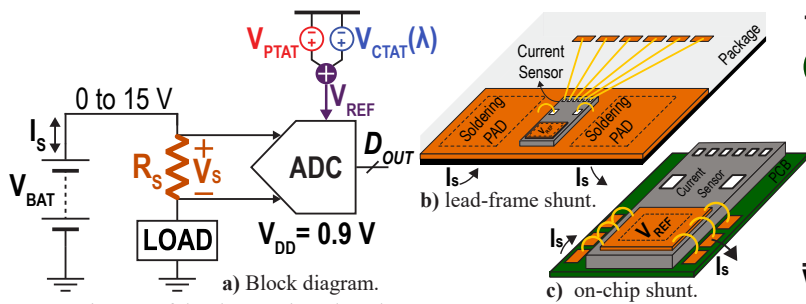


Fig. 1: Diagram of the shunt resistor-based current sensor system.

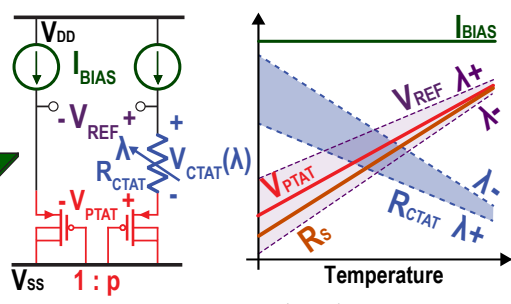


Fig. 2: Temperature compensation scheme.

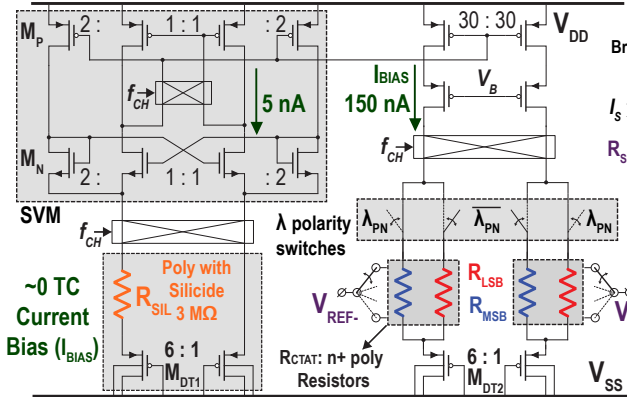


Fig. 3: V_{REF} and I_{BIAS} generation.

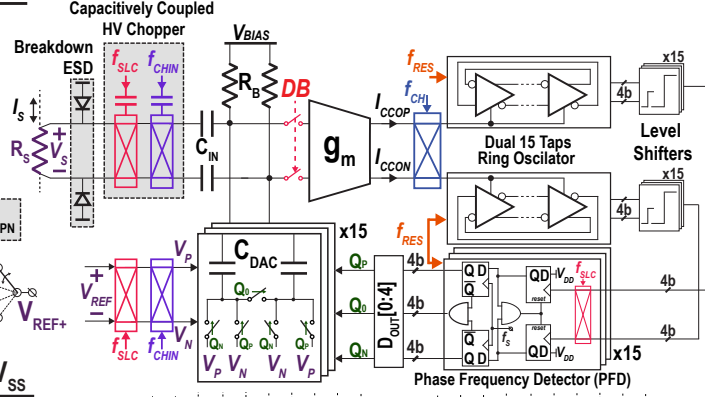


Fig. 4: Diagram of the readout circuit.

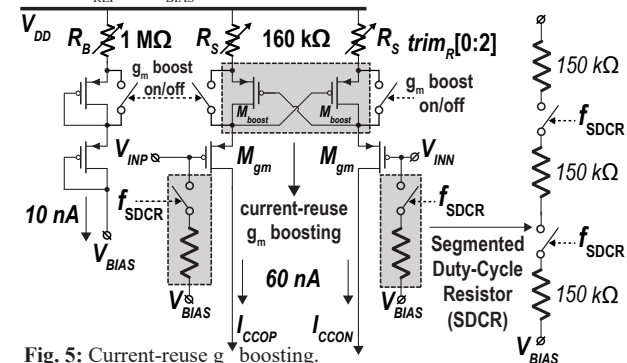


Fig. 5: Current-reuse g_m boosting.

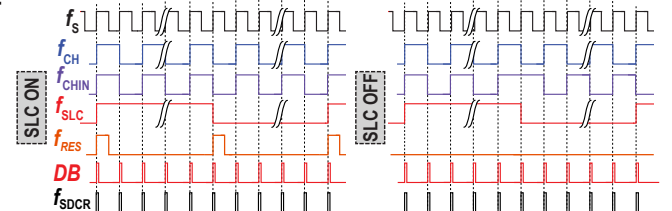


Fig. 6a: Chip micrograph.

Fig. 6b: Chip over the lead-frame

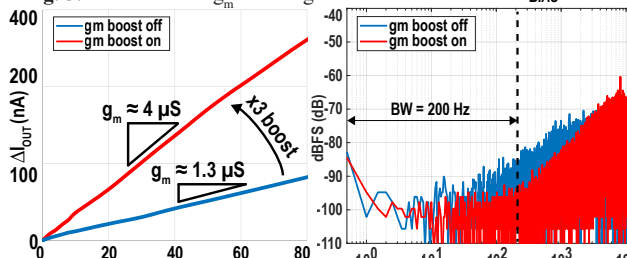


Fig. 7: g_m boost.

Fig. 8: Free running spectrum.

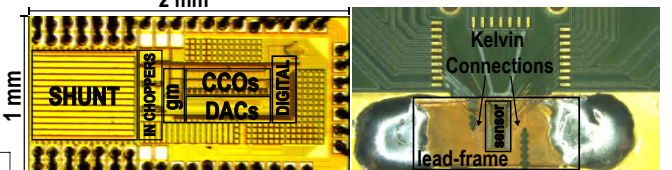


Fig. 11: I_{BIAS} vs. Temperature.

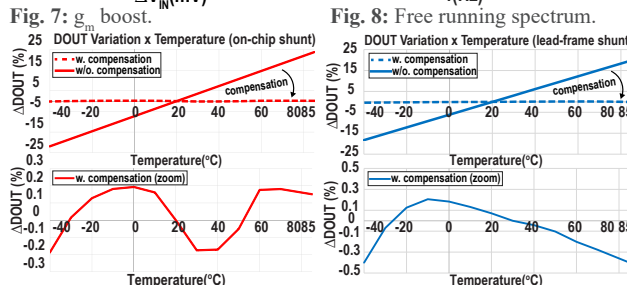


Fig. 9: DOUT variation versus temperature of a typical sample.

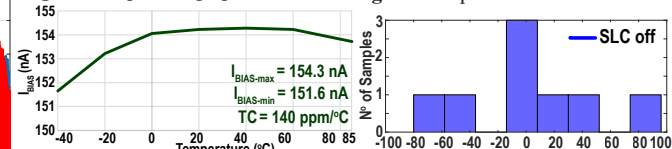


Fig. 12: Spectrum for various ICM.

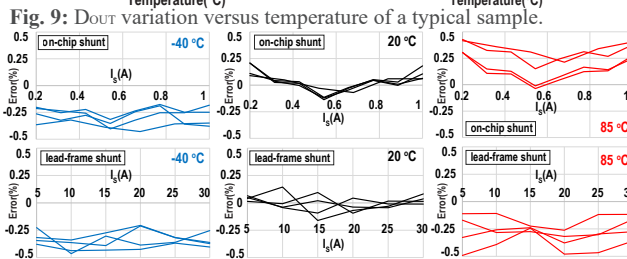


Fig. 10: Gain error.

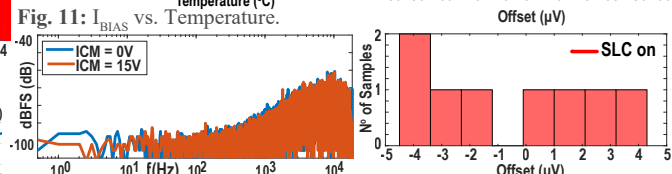


Fig. 13: Offset.

Tab. 1: Performance summary.

	This Work	ISSCC 23 [1]	VLSI 21 [2]	ISSCC 20 [3]	ISSCC 18 [4]
P_{SUPPLY}	720 nW	504 μ W	2.5 μ W	9 μ W	19.6 μ W
Shunt	on-chip 40m Ω	0.83m Ω	on-chip 20m Ω	50m Ω	10m Ω
	lead-frame 0.3m Ω	PCB Trace	PCB trace 3m Ω	low-TCR*	on-chip
IRANGE	on-chip \pm 1A	\pm 40A	on-chip \pm 2A	\pm 1A	\pm 4A
	lead-frame \pm 30A		PCB trace \pm 15A		
Gain Error	on-chip \pm 0.5%	\pm 0.2%	on-chip \pm 0.35%	\pm 0.5%*	\pm 0.9%
Offset	on-chip 5 μ V	4 μ V	500nV	1 μ V	400nV
	ICMR 0 to 15V	low-side	-0.3 to 5 V	0 to 60 V	0 to 25 V
Tech.	0.18	0.18	0.18	0.18 BCD	0.18 BCD
V_{SUPPLY}	0.9V	1.8 V	1.8 V	1.7V	1.5V
T_{RANGE}	-40 to 85°C	-50 to 125°C	-40 to 85°C	-50 to 125°C	-40 to 85°C
Resolution	4 μ V _{RMS}	1.4 μ V _{RMS}	5.4 μ V _{RMS}	-	1.5 μ V _{RMS}
T_{CONV}	5ms	0.1ms	16ms	-	2ms
FOM**	164dB	160dB	149dB	-	162dB

* Uses a custom/off-chip low-TCR shunt

** FoM=Dynamic Range + 10log(Bandwidth/Power)